



# The Critical Role of Galactic Dynamics in Regulating the Spatial Structure, Kinematics, and Star Formation Activity of Clouds in the Central Molecular Zone

**Diederik Kruijssen**

Heidelberg University  
[kruijssen@uni-heidelberg.de](mailto:kruijssen@uni-heidelberg.de)  
[www.mustang-project.org](http://www.mustang-project.org)

*The evolution of molecular clouds in galactic centres is thought to differ from that in galactic discs due to a significant influence of the external gravitational potential. We present a set of numerical simulations of molecular clouds orbiting on the 100-pc stream of the Central Molecular Zone (CMZ; the central ~500 pc of the Galaxy) and characterise their morphological and kinematic evolution in response to the background potential and eccentric orbital motion.*

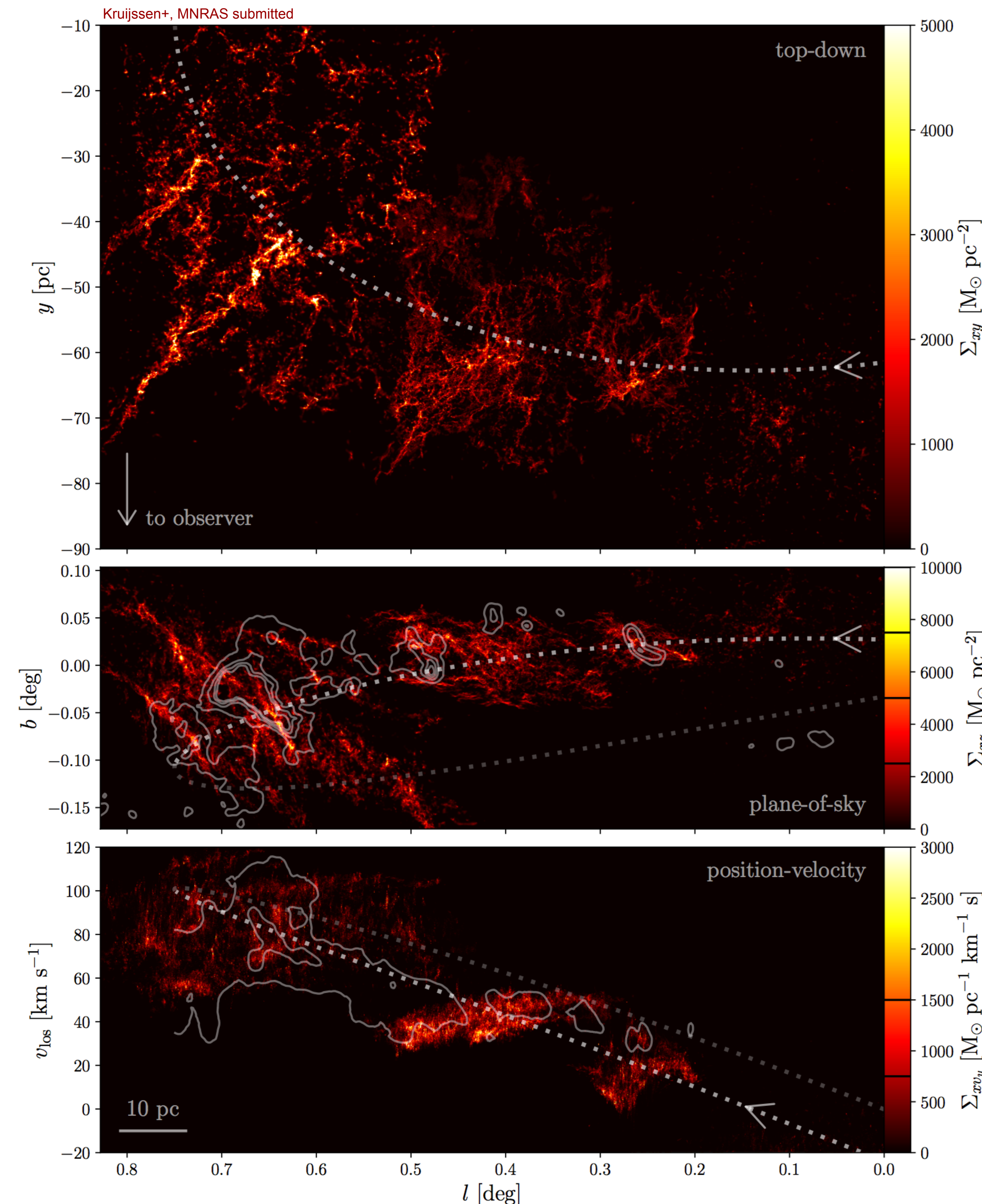


**Figure 2.** Combined column density maps of the simulations at several different snapshots, chosen to best represent the observed clouds on the CMZ ‘dust ridge’ (see the text). The orbital solution of Kruijssen et al. (2015) is shown as the light grey line, with the segment thereof covered by the simulations shown in a brighter shade and arrows indicating the direction of motion. Top panel: top-down projection. Middle panel: plane-of-sky projection. For comparison, the observed column density map of the gas traced by cold dust (from HiGAL, see Battersby et al. in prep.) is shown by contours at  $\Sigma_{xz} = \{2.5, 5, 7.5, 10\} \times 10^3 \text{ M}_{\odot} \text{ pc}^{-2}$  (black lines in the colour bar). Bottom panel: position-velocity projection. This figure shows that the main morphological and kinematic features of the observed dust ridge clouds can be reproduced by drawing a population of clouds from the initial conditions appropriate for the CMZ listed in Table 1 and simulating their dynamical evolution in the gravitational potential of the CMZ. For comparison, the observed position-velocity distribution of the molecular gas in the dust ridge traced by  $^{13}\text{CO}(2-1)$  (Ginsburg et al. 2016) is shown by contours at  $\Sigma_{xv_y} = \{0.75, 1.5\} \times 10^3 \text{ M}_{\odot} \text{ pc}^{-1} \text{ km}^{-1} \text{ s}$  (black lines in the colour bar). An animated version of this figure is available at the link given by the QR code.

## A simulated Brick: the Archetype of a YMC progenitor cloud reproduced by self-consistently modelling its hydrodynamics in the gravitational potential of the CMZ

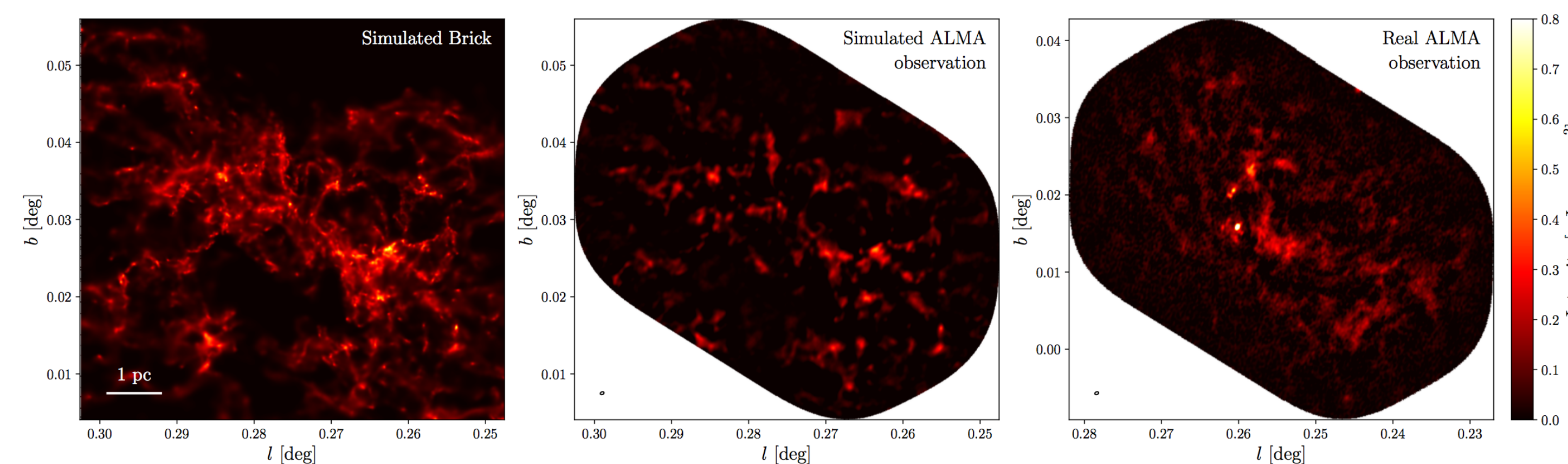


**Figure 6.** Comparison of dust continuum observations of the ‘Brick’ obtained with ALMA at 3 mm (89 GHz) to a simulated observation of the high-density simulation at the same position as the real Brick. Panel 1: column density map of the native simulation, restricted to the high-density part of the gas reservoir associated with the cloud. Panel 2: simulated observation of panel 1, mimicking the precise setup of the ALMA observations. Panel 3: real ALMA observation from Rathborne et al. (2015). All maps are scaled to the same units as indicated by the colour bar and described in the text. The ellipse in the bottom-left corners of panels 2 and 3 illustrates the beam shape and size. This figure shows that the morphology and typical peak brightness of the simulated cloud are similar to those of the observed Brick.

We argue that the accretion of gas clouds onto the central regions of galaxies, where the rotation curve turns over and the tidal field is fully compressive, is accompanied by transformative dynamical changes to the clouds, leading to collapse and star formation (Figure 10). This can generate an evolutionary progression of cloud collapse with a common starting point, which either marks the time of accretion onto the tidally-compressive region or of the most recent pericentre passage. Together, these processes may naturally give rise to the synchronised starbursts observed in numerous (extra)galactic nuclei.

Interested? Both papers are currently submitted to MNRAS and will be on astro-ph soon.

## The dynamical evolution of molecular clouds near the Galactic Centre – II. Spatial structure and kinematics of simulated clouds

J. M. D. Kruijssen,<sup>1,2\*</sup> J. E. Dale,<sup>3</sup> S. N. Longmore,<sup>4</sup> D. L. Walker,<sup>5,6</sup> J. D. Henshaw,<sup>2</sup> A. Ginsburg,<sup>7</sup> S. M. R. Jeffreson,<sup>1</sup> A. T. Barnes,<sup>4,8</sup> C. D. Battersby,<sup>9</sup> K. Immer,<sup>10</sup> J. M. Jackson,<sup>11</sup> E. R. Keto,<sup>12</sup> N. Krieger,<sup>2</sup> E. A. C. Mills,<sup>13</sup> Á. Sánchez-Monge,<sup>14</sup> A. Schmiedeke,<sup>8</sup> S. T. Suri<sup>14</sup> and Q. Zhang<sup>12</sup>

## The dynamical evolution of molecular clouds near the Galactic Centre – III. Tidally-induced star formation in protocluster clouds

James E. Dale<sup>1</sup>, J. M. Diederik Kruijssen<sup>2</sup> and S. N. Longmore<sup>3</sup>

**Table 1.** Initial conditions of the simulations.

Simulation	$M$	$R_t$	$\sigma$	$\alpha_{\text{vir}}$	$\rho$	$\Sigma$	$t_{\text{ff}}$
fiducial	7.7	13.6	24.1	9.4	1.3	1.3	0.94
low density	13.4	23.5	41.2	27.4	0.4	0.8	1.63
high density	4.5	7.8	13.9	3.1	3.8	2.3	0.54
low vel. disp.	1.0	6.8	12.1	9.4	1.3	0.7	0.94
high vel. disp.	26.1	20.4	36.2	9.4	1.3	2.0	0.94

Note: All listed quantities are evaluated over the full volume of the clouds, i.e. out to the truncation radius  $R_t$ , which is about 1.7 times the half-mass radius. Units:  $M$  in  $10^5 \text{ M}_{\odot}$ ,  $R_t$  in pc,  $\sigma$  in  $\text{km s}^{-1}$ ,  $\rho$  in  $10^3 \text{ cm}^{-3}$ ,  $\Sigma$  in  $10^3 \text{ M}_{\odot} \text{ pc}^{-2}$ , and  $t_{\text{ff}}$  in Myr.

We find that the clouds are shaped by **strong shear**, by **tidal and geometric deformation**, and by their passage through the **orbital pericentre**. Within our simulations, these mechanisms control cloud sizes, aspect ratios, position angles, filamentary structure, column densities, velocity dispersions, line-of-sight velocity gradients, angular momenta, and kinematic complexity. By comparing these predictions to observations of clouds on the Galactic Centre ‘dust ridge’ (Figures 2, 5, and 6), we find that our simulations naturally reproduce a remarkably broad range of key observed morphological and kinematic features, which can be explained in terms of well-understood physical mechanisms.

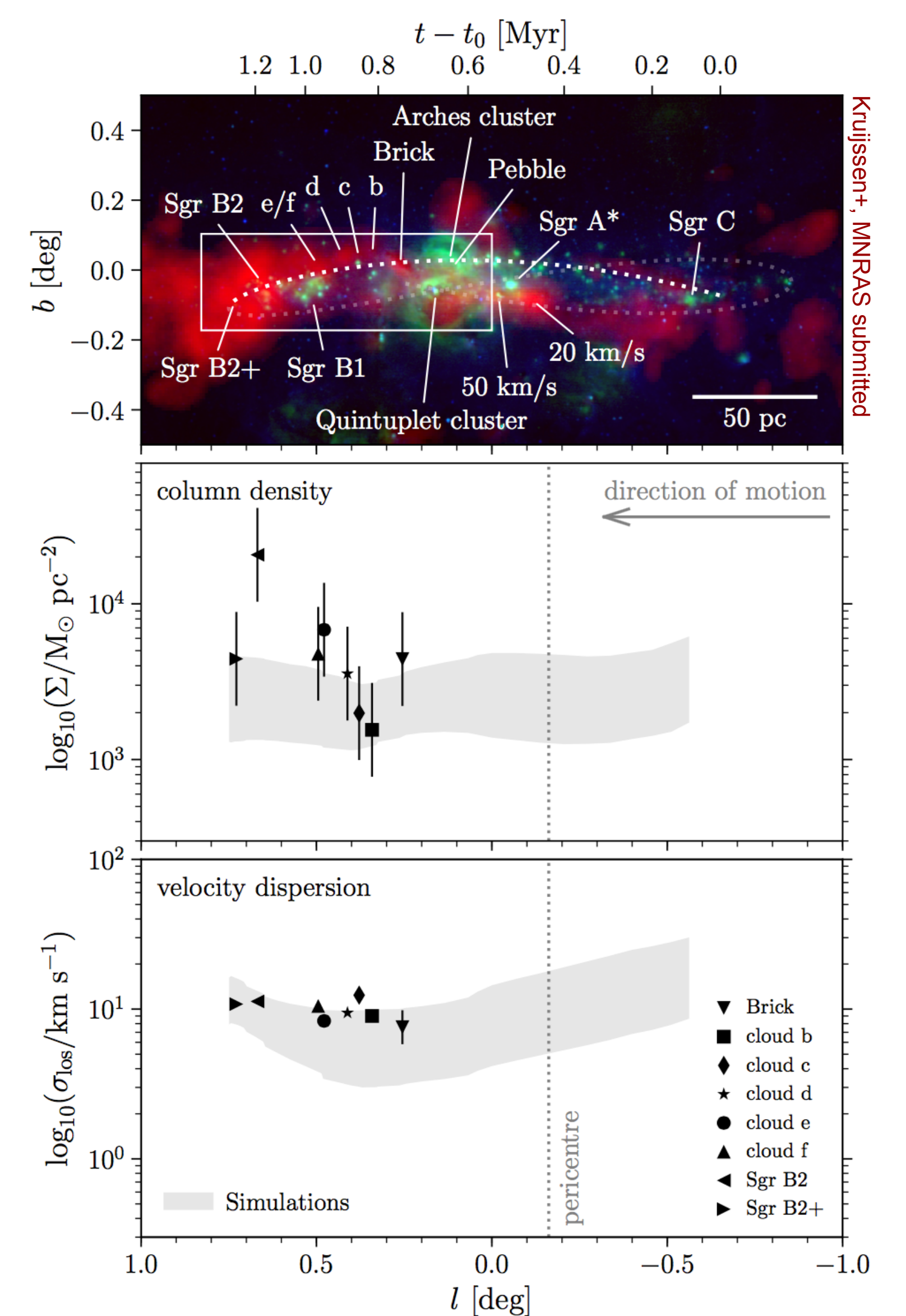


**Figure 5.** Comparison of the simulations to observed dust ridge clouds. Panel 1: three-colour composite image of the CMZ. Panel 2: column densities. Panel 3: line-of-sight velocity dispersions. The symbols represent the observed properties of the dust ridge clouds, whereas the grey-shaded area indicates the range spanned by the simulated clouds for the five different initial conditions from Table 1. For the models, the column densities and velocity dispersions are calculated in the same way as in observational studies, such that the comparison is appropriate. They are also averaged over a 0.3 Myr time window to reduce stochasticity. This figure shows that most of the observed column densities and velocity dispersions of dust ridge clouds are reproduced by drawing from the range of cloud properties observed upstream and simulating their evolution. Only the column density of Sgr B2 exceeds the range covered by the simulations.

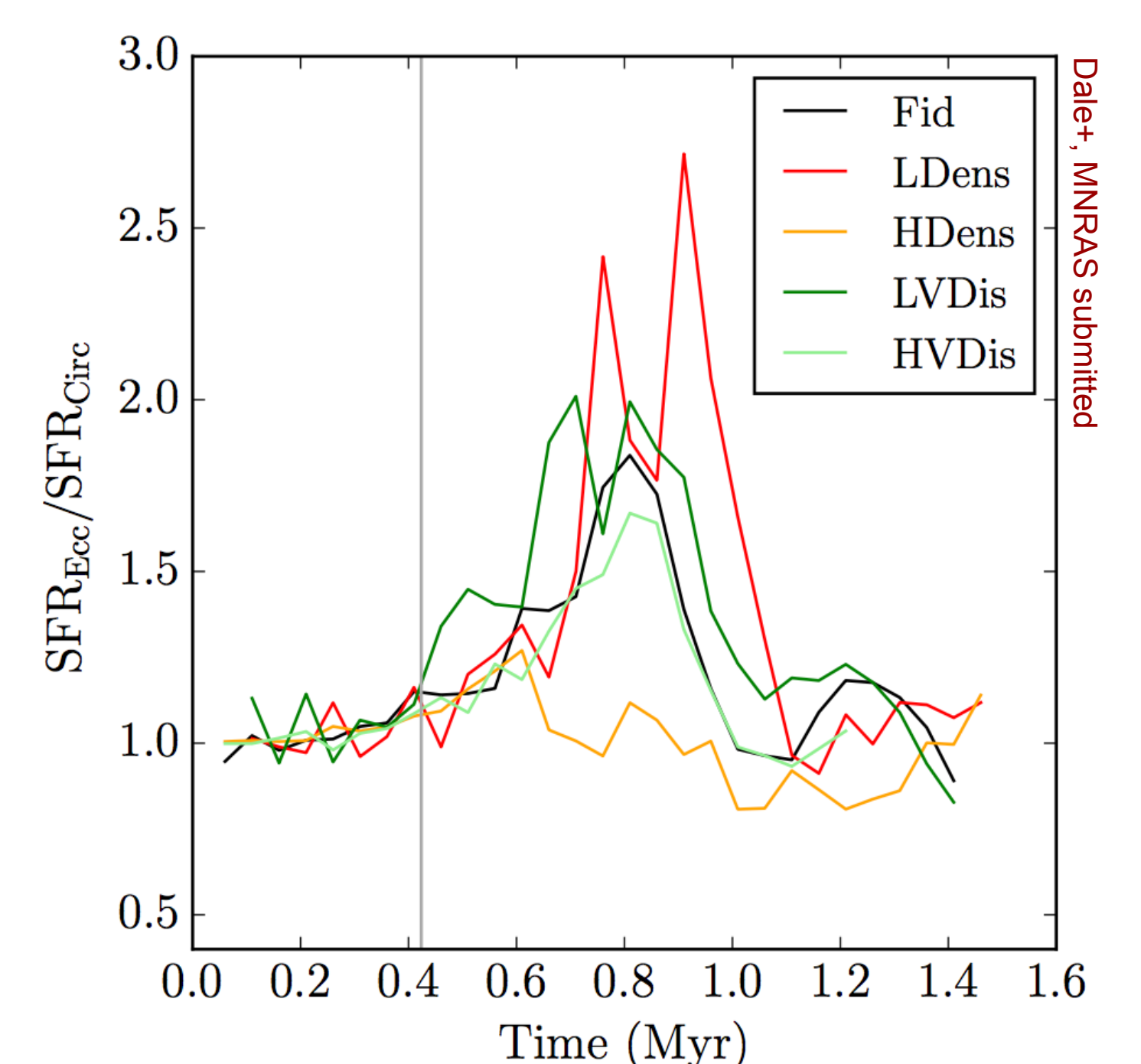


**Figure 10.** Time evolution of the star formation rates of the tidally-virialised clouds on eccentric relative to those on circular orbits.